

# LEGIBILITY NOTICE

A major purpose of the Technical Information Center is to provide the broadest dissemination possible of information contained in DOE's Research and Development Reports to business, industry, the academic community, and federal, state and local governments.

Although a small portion of this report is not reproducible, it is being made available to expedite the availability of information on the research discussed herein.

CONF-900450--1

LA-UR--90-1630

DE90 011974

TITLE GLOBAL NUCLEAR-STRUCTURE CALCULATIONS

AUTHOR(S): Peter Moller and J. Rayford Nix

SUBMITTED TO For presentation at the Conference on Nuclear Structure in the Nineties, Oak Ridge, Tennessee, April 23-27, 1990

DISCLAIMER

This report was prepared as an account of work sponsored by an agency of the United States Government. Neither the United States Government nor any agency thereof, nor any of their employees, makes any warranty, express or implied, or assumes any legal liability or responsibility for the accuracy, completeness, or usefulness of any information, apparatus, product, or process disclosed, or represents that its use would not infringe privately owned rights. Reference herein to any specific commercial product, process, or service by trade name, trademark, manufacturer, or otherwise does not necessarily constitute or imply its endorsement, recommendation, or favoring by the United States Government or any agency thereof. The views and opinions of authors expressed herein do not necessarily state or reflect those of the United States Government or any agency thereof.

By acceptance of this article, the publisher recognizes that the U.S. Government retains a nonexclusive, royalty-free license to publish or reproduce the published form of this contribution, or to allow others to do so, for U.S. Government purposes.

The Los Alamos National Laboratory requests that the publisher identify this article as work performed under the auspices of the U.S. Department of Energy.

Los Alamos Los Alamos National Laboratory Los Alamos, New Mexico 87545

119

# **Global Nuclear-Structure Calculations**

**Peter Möller and J. Rayford Nix**

**April 20, 1990**

**For presentation at the  
Conference on Nuclear Structure in the Nineties  
Oak Ridge, Tennessee, April 23-27, 1990**

# GLOBAL NUCLEAR-STRUCTURE CALCULATIONS

Peter MÖLLER and J. Rayford NIX

Theoretical Division, Los Alamos National Laboratory, Los Alamos, NM 87545

**Abstract:** The revival of interest in nuclear ground-state octupole deformations that occurred in the 1980's was stimulated by observations in 1980 of particularly large deviations between calculated and experimental masses in the Ra region, in a global calculation of nuclear ground-state masses. By minimizing the total potential energy with respect to octupole shape degrees of freedom in addition to  $\epsilon_2$  and  $\epsilon_4$  used originally, a vastly improved agreement between calculated and experimental masses was obtained. To study the global behaviour and interrelationships between other nuclear properties, we calculate nuclear ground-state masses, spins, pairing gaps and  $\beta$ -decay half-lives and compare the results to experimental quantities. The calculations are based on the macroscopic-microscopic approach, with the microscopic contributions calculated in a folded-Yukawa single-particle potential.

## 1. Introduction

Theoretical studies based on single-particle models and its various extensions, such as the macroscopic-microscopic method and RPA treatments of additional residual interactions, have over the last 40 years been enormously successful in providing a quantitative theoretical interpretation of a large number of different low-energy nuclear-structure properties. In the early 1950's the nuclear magic numbers were explained in terms of a simple spherical single-particle model with a spin-orbit interaction with an adjustable spin-orbit strength. In 1955 Nilsson<sup>1)</sup> extended the model to a deformed single-particle well and this model was very successful in interpreting a vast amount of experimental low-energy spectroscopic data.

The single-particle model serves as a starting point in the macroscopic-microscopic method for calculating the nuclear potential energy as a function of shape. To obtain the potential energy in this approach, a macroscopic energy is calculated in a model such as the liquid-drop model for the shape of interest, single-particle levels are calculated for a well of this shape and used to determine a microscopic shell correction by use of Strutinsky's method<sup>2)</sup>. The total potential energy is then obtained as the sum of the macroscopic term plus microscopic shell and pairing corrections. By calculating the potential energy for a large number of shapes one may determine nuclear ground-state shapes and masses, fission barriers and fission isomeric states. At this conference we will also hear about how the macroscopic-microscopic approach has been extended to studies of high-spin phenomena.

The single-particle model also serves as a starting point for calculating various transition-rate nuclear matrix elements. One example of extensive studies of this type is the modelling of Gamow-Teller  $\beta$ -strength functions. Since the transition amplitude is sensitive to small perturbations from residual interactions it is necessary to add a residual pairing and a residual Gamow-Teller interaction to the basic single-particle model to obtain reasonable agreement with data.

The goal of theoretical studies of the above type is to understand experimentally observed properties of nuclei in terms of a simple underlying physical picture. Usually a model can be characterized as providing such a simple underlying physical picture only if it has relatively few parameters. Although few-parameter models often exhibit larger deviations between calculated results and data than multi-parameter models do, these deviations are often open to

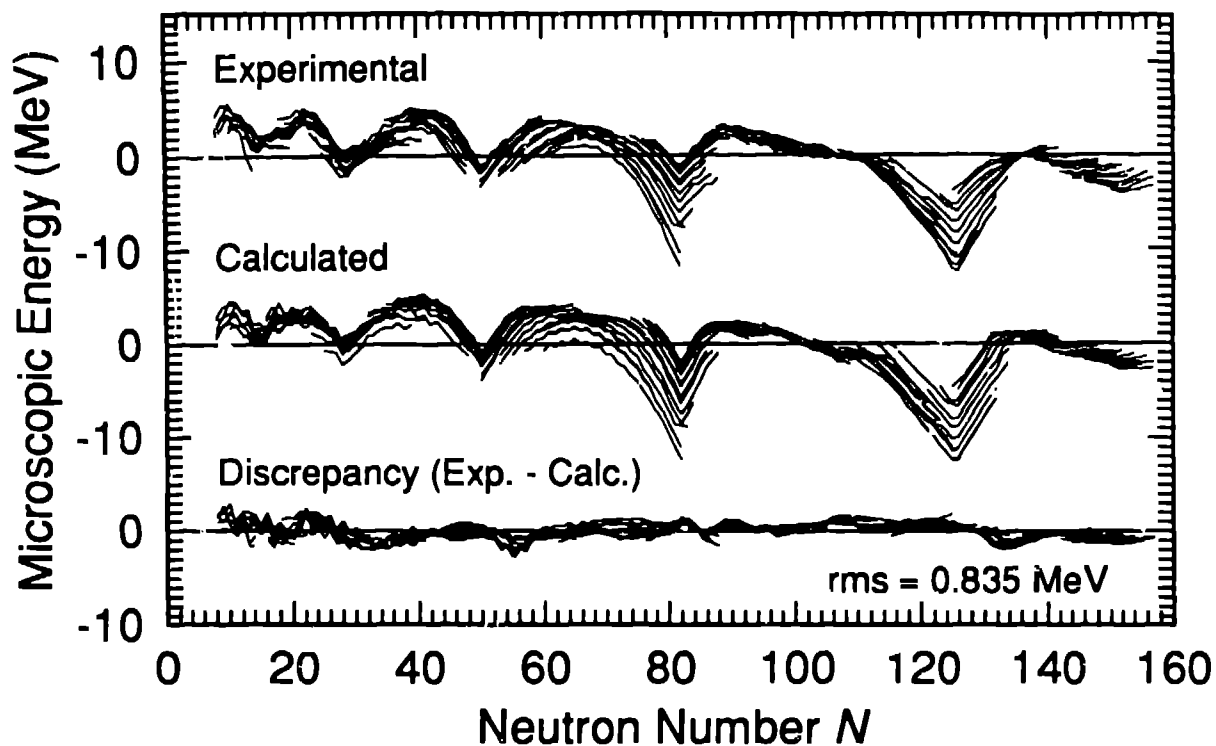


Figure 1: Difference between experimental and calculated ground-state masses (bottom part of figure). The deviations at about  $N = 132$  are mostly removed by considering octupole shape degrees of freedom when minimizing the potential energy.

interpretations that yield new physical insight. The deviations may, for example, be due to a known approximation in the model or reveal a previously unsuspected phenomenon.

The model used here represents a unified macroscopic-microscopic approach with about 10 parameters in the macroscopic part and 10 in the single-particle model, not counting obvious parameters such as the proton and neutron mass, Planck's constant, the speed of light, etc. Our aim here is to show some remarkable strengths and some weaknesses of these single-particle-based models by applying them globally to calculations of such diverse properties as ground-state masses, deformations, spins and pairing effects,  $\beta$ -decay properties, fission-barrier structure and spontaneous-fission half-lives.

## 2. Calculated results

### 2.1. GROUND-STATE MASSES

At this session and at this conference it is particularly appropriate for us to show the comparison between calculated nuclear ground-state masses and experimental data in fig. 1. This figure represents the results of our first global calculation<sup>3,4)</sup> of nuclear-structure properties, in which microscopic effects were taken into account. Experimental and calculated single-particle corrections are shown in the top two portions of the figure, and their difference, which is also the difference between calculated and experimental masses, is shown in the bottom part.

The figure is appropriate for this session because we realized that the unusually large deviations centered around  $^{223}\text{Ra}$  could possibly be removed by minimizing the potential energy with respect to shape degrees of freedom in addition to the  $\epsilon_2$  and  $\epsilon_4$  parameters that were considered in the calculation shown in fig. 1. It was natural to consider octupole shape degrees of

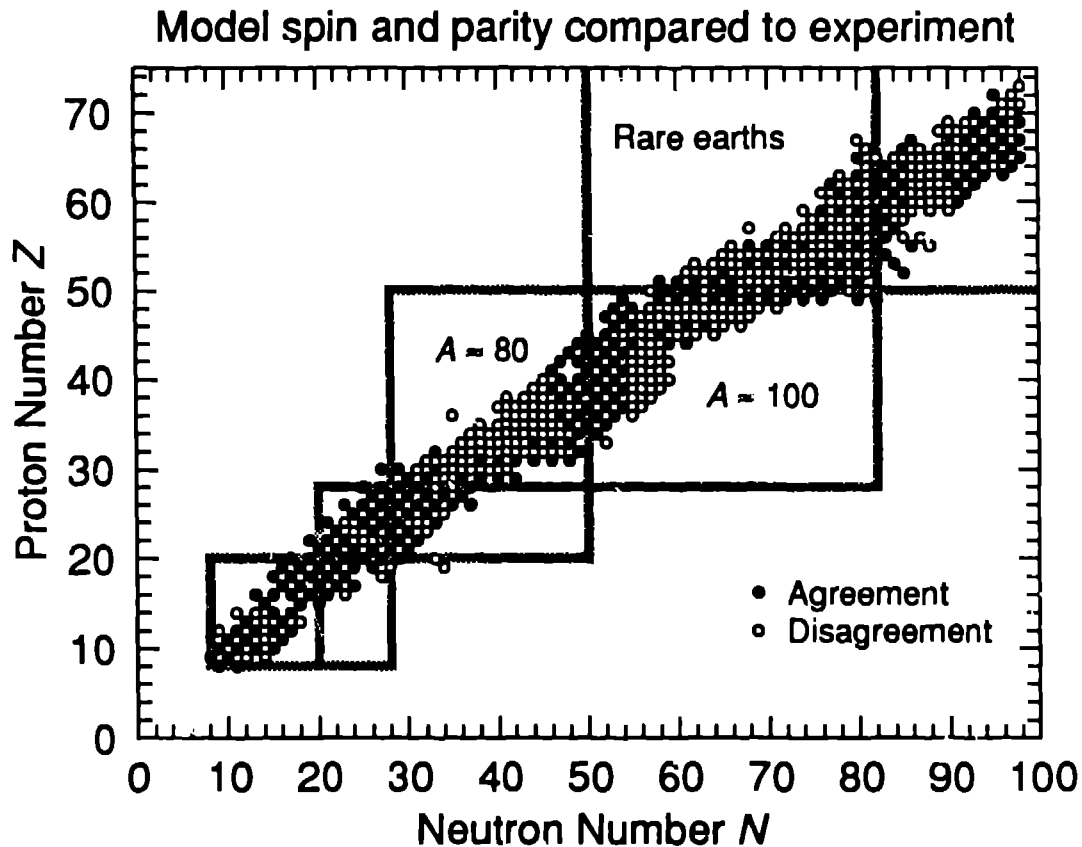


Figure 2: Comparison of calculated and experimental nuclear ground-state spins for odd-even nuclei. Spherical spin assignments are used in the calculations when  $|\epsilon_2| < 0.15$ . Many of the discrepancies occur where several levels are grouped close together.

freedom because of the low-lying negative-parity states in this region, and our initial study<sup>3)</sup> clearly showed that the octupole degree of freedom almost entirely removed the discrepancy between the calculated and experimental masses in the vicinity of  $^{222}\text{Ra}$ . In the heavy-actinide region the  $\epsilon_6$  shape degree of freedom lowers the ground-state mass by up to 1 MeV close to  $^{252}\text{Fm}$ , which decreases the discrepancy beyond Pb to almost zero.

The figure is also appropriate in the larger context of this conference, dedicated to the memory of George Leander. When he learned of these results, very shortly after they were obtained, he jumped on the bump in the Ra region, and with characteristic energy and enthusiasm he immediately suggested a large variety of calculations that should be undertaken. When one of us (PM) cautioned that it would be a little difficult because the codes that were initially required ran only on computers at the Los Alamos National Laboratory, he very simply overcame this obstacle by going to Los Alamos and performing the calculations there. His first visit to this Laboratory led to one of his first papers<sup>4)</sup> in his long string of publications on this subject.

## 2.2. GROUND-STATE SPINS

The most important parameters in the folded-Yukawa single-particle model are the diffuseness and spin-orbit parameters, which were determined<sup>6)</sup> in 1974 in the rare-earth and actinide regions from comparisons between calculated and experimental single-particle level ordering. The global nuclear-mass study<sup>3)</sup> in 1981 introduced a parameter set valid for the entire nuclear chart in terms of an expression for the spin-orbit parameter that is linear in  $A - N + Z$ , with the expression fully defined by the previously determined parameter val-

### Model spin and parity compared to experiment

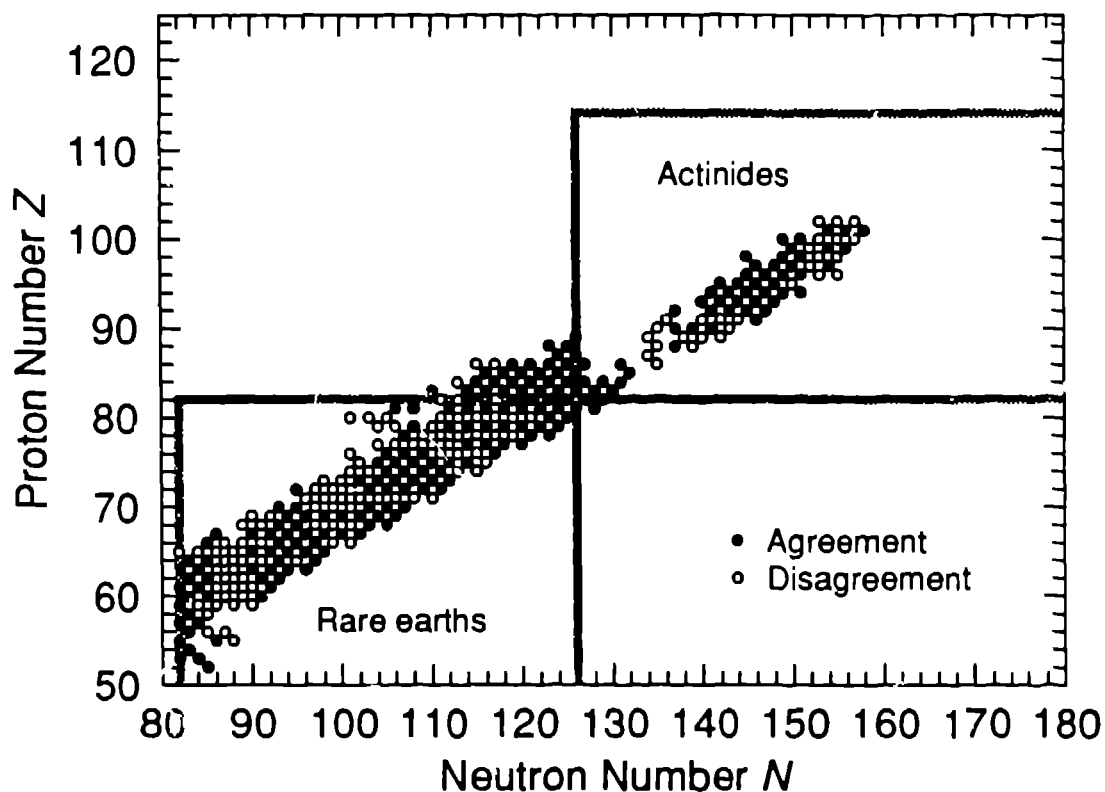


Figure 3: Similar to fig. 2, but for the heavy region. The discrepancies in the beginning of the actinide region are mostly removed by minimizing the potential energy also with respect to octupole shape degrees of freedom.

ues in the actinide and rare-earth regions. The parameter-determination procedure is fairly subjective, because it is not based on exact comparisons between all available data and calculations. Instead, it typically proceeds by calculating single-particle level diagrams as functions of deformation for several parameter sets, comparing their structure to a few selected nuclei and forming an opinion on which of the parameter sets gives the best agreement.

Because we now have available nuclear ground-state shapes from our calculations of ground-state masses, we are in a position to compare calculated and experimental ground-state spins in a well-defined manner, as shown in figs. 2 and 3. The only ambiguity is how to compare the spins for nuclei calculated to be weakly deformed. We have chosen to base the comparison on spherical assignments if  $|\epsilon_3| < 0.15$  in the calculations. With this rule we obtain agreement in 428 cases and disagreement in 285 cases, corresponding to 60% agreement. This result is not very sensitive to changes in the rule concerning when to use spherical assignments. In fact, if we *always* choose spherical assignment if this choice yields agreement with data we obtain agreement in about 450 case and disagreement in 248 cases, so that the improvement in the agreement is only 4%. The disagreements between the calculated and experimental spins usually arise because several deformed or spherical levels lie very close together, making accurate calculations difficult. For magic numbers there is an almost stunning agreement, which, taken together with our analysis of the disagreements in other regions, makes it unlikely that a significantly better global parameter set can be found. The existing disagreements probably have to be explained in terms of residual interactions outside the framework of the single-particle model.

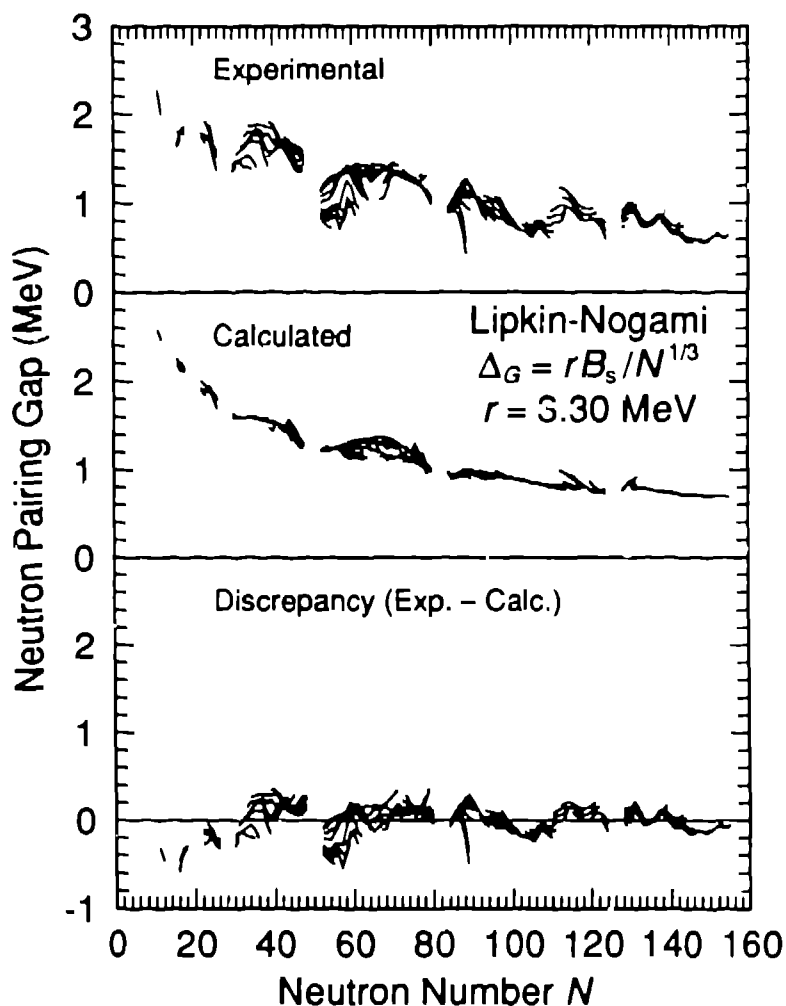


Figure 4: Neutron pairing gaps calculated in the Lipkin-Nogami approximation, with an optimized effective-interaction pairing gap  $\Delta_G$ , compared to experimental odd-even mass differences. Much of the discrepancy probably arises because the odd-even mass differences do not yield precisely the pairing gap. The two large discrepancies at  $N \approx 90$  are probably due to errors in experimental masses.

### 2.3. PAIRING GAPS

The nuclear pairing residual interaction exerts a powerful influence on nuclear ground-state properties. Recently, several investigations have suggested an isospin dependence of the average pairing gap, specifically a decrease of the pairing gap with neutron excess. In a more detailed analysis<sup>7)</sup> we have found that for meaningful statements on the dependence of nuclear pairing properties on neutron excess one must distinguish between the pairing gap that is *observed* through odd-even mass differences, and the *effective-interaction* pairing gap  $\Delta_G$ . From the latter quantity the pairing constant  $G$  used in microscopic models can be determined throughout the periodic system. We have calculated microscopic pairing gaps for about 1400 nuclear ground states for sufficiently many parameter sets of the effective-interaction pairing gap  $\Delta_G$  to perform least-squares minimizations of the deviations between the calculated pairing gaps and experimental pairing gaps determined from odd-even mass differences. In practice this means we have solved the microscopic pairing equations for 1400 nuclei for about 200 different parameter values. We find *no explicit isospin dependence* of the effective-interaction pairing parameters. In fact, the simple expressions



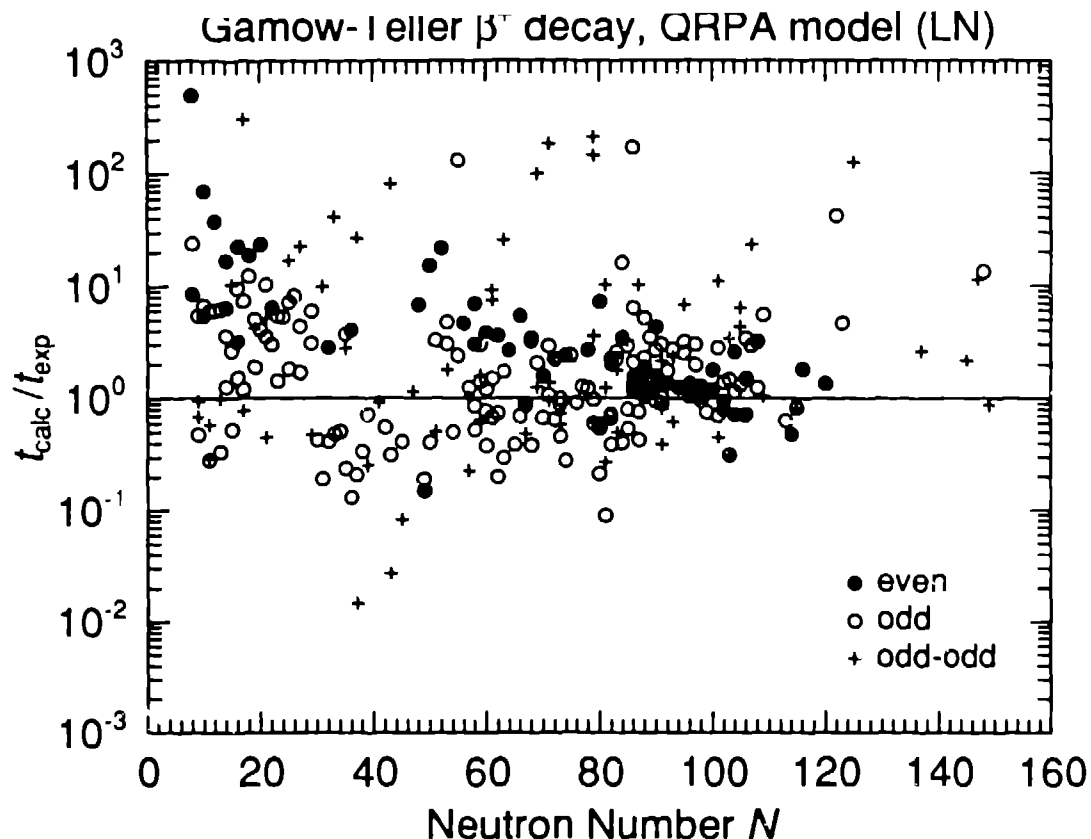


Figure 5: Calculated half-lives for  $\beta^+$  decay compared to experimental data for all known cases with  $T_{1/2}^{\text{exp}} < 100$  s. The symbols refer to the mother nucleus. As has been common practice, we have multiplied the calculated half-lives by 2, to account for the “missing strength,” but as discussed in the text these calculations show no evidence of missing strength.

$$\Delta_G = \tau B_s / N^{1/3} \text{ for neutrons and} \quad \Delta_G = \tau B_s / Z^{1/3} \text{ for protons}$$

where  $B_s$  is the surface area of the deformed nucleus relative to spherical shape represent our final result<sup>7)</sup>. The single parameter has the value  $\tau = 3.30$  MeV in the Lipkin-Nogami approximation<sup>8,9)</sup> and  $\tau = 4.80$  MeV in the BCS approximation. An example of results obtained is shown in fig. 4. In contrast to the statement by Pradhan, Nogami and Law<sup>9)</sup> that “Anyone who has a computer programme for the usual BCS calculation can readily do the LN calculation . . .” we found that designing a fast computer program that would reliably converge in millions of calculations with *realistic* single-particle spectra, as contrasted to the two-level model investigated in ref. <sup>9)</sup>, was a formidable task. In this effort we received frequent and crucial advice from Leander and Nazarewicz, who had initially motivated us to investigate the Lipkin-Nogami approximation as an alternative to the BCS approximation.

#### 2.4. $\beta$ -STRENGTH FUNCTIONS

Gamow-Teller nuclear  $\beta$ -decay strength functions often depend characteristically on the deformation of the decaying system<sup>10,11)</sup>, with a few strong peaks present for spherical nuclei, but with a more spread-out appearance for deformed nuclei. We have based a calculation of  $\beta$ -decay half-lives for all experimentally known nuclei with  $T_{1/2}^{\text{exp}} < 100$  s on a model<sup>11,12)</sup> that constructs the wave functions of the mother and daughter nuclei by considering deformed single-particle wave functions as the starting point, adding pairing and Gamow-Teller residual interactions and treating the problem in the Quasi-particle RPA approximation (QRPA). We

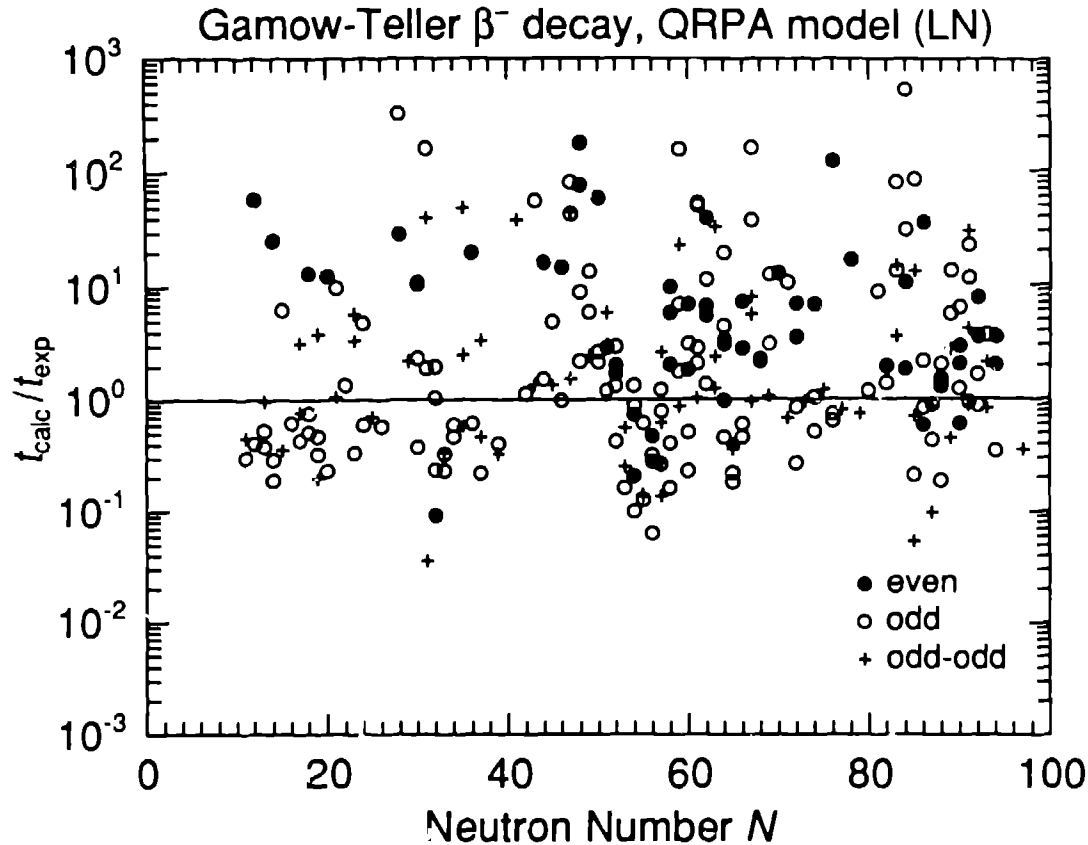


Figure 6: Similar to fig. 5 but for  $\beta^-$  decay. Because less than 10 nuclei with  $T_{1/2}^{\text{exp}} < 100$  s are known for  $N > 100$  the plot was terminated at  $N = 100$  for greater clarity.

display the first global results we have obtained in this model in figs. 5 and 6 for  $\beta^+$  and  $\beta^-$  decay, respectively. The calculation is based on folded-Yukawa wave functions and the Lipkin-Nogami pairing model, where the preliminary value  $\Delta_G = 9.0 \text{ MeV}/A^{1/2}$  value was used. Following conventional practice<sup>11,12</sup>) we have “renormalized” the calculated strength by dividing the model results by 2. We find, roughly, that the centroid of the distribution of the ratio  $t_{\text{calc}}/t_{\text{exp}}$  is about 4 for the even-even case, and about 2 for the two odd cases. The number of even cases in each plot is about 50 and the number of the odd and odd-odd cases is about 200. Thus, a renormalization of the strength seems unwarranted. The spread of the distributions around the centroids range from about a factor of 4 to about a factor of 8, with the smallest spread obtained for the even-even cases. We are still in the process of interpreting these results. While we were generalizing the  $\beta$ -strength programs to accept folded-Yukawa wave functions as input, we received, naturally, advice to shortcuts from George Leander: “Why don’t you use the code I wrote for Woods-Saxon wave functions? I think you use the same basis functions in the folded-Yukawa program, so you can probably use it without much modification.” This helpful advice saved us considerable time.

## 2.5. ASTROPHYSICAL APPLICATIONS

Finally, we illustrate the importance of global nuclear-structure calculations for astrophysical applications. In fig. 7 we show the difference between calculated  $\beta$ -decay energies and fission-barrier heights for actinide nuclei. In the gray regions the  $Q$  value of the  $\beta$  decay exceeds the fission-barrier height, and  $\beta$ -delayed fission is possible in the decay from the  $r$ -process line to the line of  $\beta$  stability. However, detailed calculations<sup>13</sup>) show that this decay mode is of minor importance.

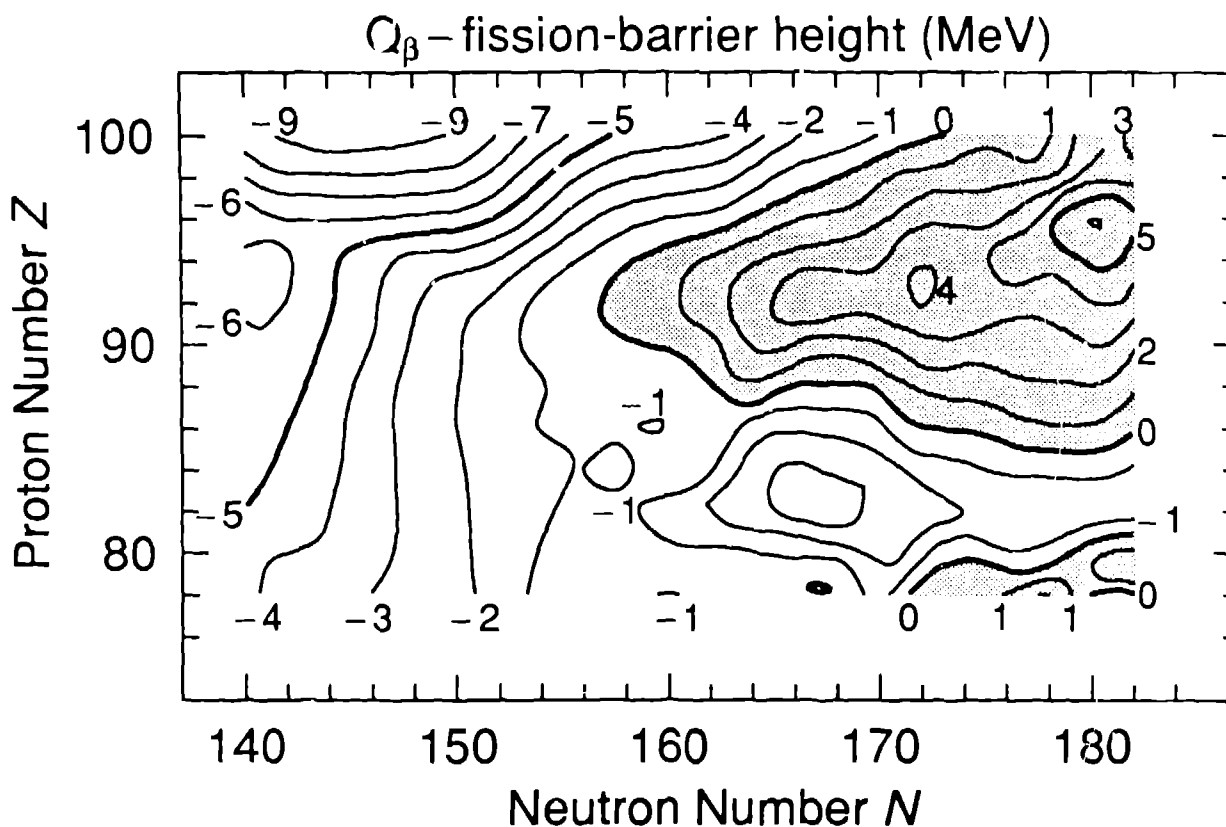


Figure 7: Difference between maximum energy release in  $\beta^-$  decay and calculated fission-barrier heights. When the energy release in  $\beta$  decay is larger than the fission-barrier height  $\beta$ -delayed fission is possible, indicated by the shaded areas.

#### References

- 1) S. G. Nilsson, Kgl. Danske Videnskab. Selskab. Mat.-Fys. Medd. **29**:No. 16 (1955)
- 2) V. M. Strutinsky, Nucl. Phys. **A95** (1967) 420; **A122** (1968) 1.
- 3) P. Möller and J. R. Nix, Nucl. Phys. **A361** (1981) 117.
- 4) P. Möller and J. R. Nix, Atomic Data Nucl. Data Tables **26** (1981) 165.
- 5) G. A. Leander, R. K. Sheline, P. Möller, P. Olanders, I. Ragnarsson, and A. J. Sierk, Nucl. Phys. **A429** (1982) 269.
- 6) P. Möller, S. G. Nilsson, and J. R. Nix, Nucl. Phys. **A229** (1974) 292.
- 7) P. Möller and J. Nix, Nucl. Phys. **A**, to be published.
- 8) Y. Nogami, Phys. Rev. **134** (1964) B313.
- 9) H. C. Pradhan, Y. Nogami, and J. Law, Nucl. Phys. **A201** (1973) 357.
- 10) K.-L. Kratz, Nucl. Phys. **A417** (1984) 447.
- 11) J. Krumlinde and P. Möller, Nucl. Phys. **A417** (1984) 419.
- 12) P. Möller and J. Randrup, Nucl. Phys. **A** (1990), to be published.
- 13) B. S. Meyer, W. M. Howard, G. J. Mathews, K. Takahashi, P. Möller, and G. A. Leander, Phys. Rev. **C39**, (1989) 1876.